Sensors and Materials, Vol. 38, No. 9 (2026) 5199–5214
MYU Tokyo

S & M 4618

You Only Look Once-based Detection and Counting of Blood Cells in Microscopic Smear Images with Uniform Experimental Design

Yao-Mei Chen,[1,9†] Er-Jung Hsueh,[2†] Wei-Tai Huang,[3,4*]
Meng-Hsuan Chiang,[5] Jinn-Tsong Tsai,[4,6**] and Wen-Hsien Ho[4,7,8,9,10***]

[1]School of Nursing, Kaohsiung Medical University, Kaohsiung 807, Taiwan
[2] Department of Hematology and Oncology, Yuan's General Hospital, Kaohsiung 802, Taiwan
[3]Department of Mechanical Engineering, National Pingtung University of Science and Technology, Pingtung 912, Taiwan
[4]Department of Healthcare Administration and Medical Informatics, Kaohsiung Medical University, Kaohsiung 807, Taiwan
[5]Department of Neuroradiology, E-Da Hospital, I-Shou University, Kaohsiung 824, Taiwan
[6]Department of Computer Science and Artificial Intelligence, National Pingtung University, Pingtung 900, Taiwan
[7]Department of Fragrance and Cosmetic Science, Kaohsiung Medical University, Kaohsiung, Taiwan, Kaohsiung Medical University, Kaohsiung 807, Taiwan
[8]Precision Sports Medicine and Health Promotion Center, Kaohsiung Medical University, Kaohsiung 807, Taiwan
[9]Department of Medical Research, Kaohsiung Medical University Hospital, Kaohsiung 807, Taiwan
[10]College of Professional Studies, National Pingtung University of Science and Technology, Pingtung 912, Taiwan

(Received March 4, 2026; accepted May 21, 2026)

Keywords: platelets, red blood cells, white blood cells, YOLO-based network, algorithm hyperparameter combination, uniform experimental design method

Researchers have utilized deep learning techniques, particularly object detection technology, to address the labor-intensive task of detecting and counting various blood cells in microscopic smear images. In this study, we focused on detecting and counting the three main types of blood cell: platelets, red blood cells, and white blood cells. To achieve this, a You Only Look Once (YOLO)-based network was employed, using the YOLO algorithm with its CSPDarkNet53 backbone, to automatically detect and count these blood cells. We proposed a systematic approach using the uniform experimental design method to improve the accuracy of blood cell detection and counting by optimizing algorithm hyperparameters for the YOLO-based network. By applying this optimized algorithm hyperparameter combination (OAHC) to the YOLO-based network, we enhanced the detection and counting of blood cells in the blood cell counting and detection (BCCD) dataset, resulting in the YOLO-based–OAHC model. The experimental results showed that the YOLO-based–OAHC model achieved a higher detection accuracy than the Resnet50–single shot detector model, particularly on the test set of blood cell images. The YOLO-based–OAHC model demonstrated superior accuracy in detecting and counting blood cells, particularly white blood cells and platelets, in images from the BCCD dataset.

*Corresponding author: e-mail: weitai@mail.npust.edu.tw
**Corresponding author: e-mail: jttsai@mail.nptu.edu.tw
***Corresponding author: e-mail: whho@kmu.edu.tw
†Equal contributors
https://doi.org/10.18494/SAM6321

ISSN 0914-4935

1. Introduction

A complete blood count is crucial for diagnosing various conditions, including infections, cancers, and anemia, as well as for monitoring the side effects of drugs.[1] However, medical laboratories often face the challenge of analyzing large volumes of tissue samples and blood within limited time frames. The manual counting of blood cells using laboratory equipment, hemocytometers, and chemical compounds is both time-consuming and labor-intensive. Overtime work by medical staff analyzing these samples can cause fatigue, errors, and reduced efficiency, potentially leading to severe or even fatal consequences for patients.[2] Automatically detecting and counting blood cells in images is challenging owing to the high resolution of medical images, the dense distribution of target cells, and their overlapping nature, which makes distinguishing them difficult.[3] Consequently, there is a growing need for artificial intelligence models that can automatically detect and count blood cells to enhance the accuracy and efficiency of diagnosis.

In recent years, deep learning methods have emerged as the leading approach for various computer vision tasks in medical imaging, including classification, segmentation, and object detection. Their effectiveness has been demonstrated in numerous medical image detection scenarios, such as automated studies on blood cell detection and counting,[4–6] establishing deep learning as a widely adopted technique in the field. Alam and Islam[4] introduced the You Only Look Once (YOLO) algorithm as a deep learning method for the automatic detection and quantification of three types of blood cell. The YOLO-based model was trained on modified blood smear images from the blood cell counting and detection (BCCD) dataset,[7] allowing it to accurately detect and count red blood cells (RBCs), white blood cells (WBCs), and platelets. The YOLO-based model also successfully detected and counted some unlabeled cells in the dataset, demonstrating satisfactory performance across various smear image datasets. Wang *et al.*[8] employed two advanced object detection techniques, single shot detector (SSD) and YOLO, to identify leukocytes. Leveraging the automatic feature extraction capabilities of CNNs, their approach eliminated the need for segmentation. However, it faced challenges in addressing multi-target recognition. Reena and Ameer[9] proposed a two-stage pipeline for leukocyte classification that integrates transfer learning with semantic segmentation. They utilized a pretrained network for segmenting leukocytes and employed AlexNet to classify five different types of leukocyte in peripheral blood, as shown in microscopic smear images. Drałus *et al.*[3] suggested employing the RetinaNet deep learning model to automatically detect and count three types of blood cell (platelets, WBCs, and RBCs) in microscopic smear images. The study highlighted promising outcomes while emphasizing the importance of selecting suitable confidence thresholds for accurate cell counting. Additionally, the trained model was tested on a variety of smear images to demonstrate its versatility. Chen *et al.*[10] proposed a classification method for acute lymphoblastic leukemia in microscopic images using an ensemble of ResNet101-9 models with a majority voting technique. The individual ResNet101 models in the ensemble were fine-tuned with optimized hyperparameters, which were determined using the Taguchi method. Chen *et al.*[6] utilized the Resnet50 network with an SSD to automatically detect and count various types of blood cell. They enhanced the model's accuracy by optimizing

algorithm hyperparameters using the Taguchi method. Evaluations using the BCCD dataset revealed that the Resnet50-SSD model exhibited exceptional accuracy in detecting and counting blood cells, with particular strength in identifying WBCs and RBCs.

Based on the literature review, it is evident that most studies have employed deep learning methods for blood cell classification, with only a few exploring these methods for the simultaneous detection and counting of RBCs, WBCs, and platelets.[3,4] Additionally, there is limited research on how the algorithm hyperparameter combinations impact detection accuracy within the backbone network of deep learning methods.[6,10,11] Factors such as image size, object size, and object number are crucial in determining detection accuracy and warrant further exploration in object detection research. Therefore, in this study, we aim to address the detection of multi-blood cell objects, explore the effects of image size, object size, and object number on detection accuracy, and examine the impact of algorithm hyperparameter combinations on the performance of a deep learning network.

In this study, we aimed to achieve two main objectives. First, we sought to identify the optimal algorithm hyperparameter combination for the YOLO-based network to enhance the automatic detection and counting of various blood cells. Second, we aimed to investigate the impact of image size, object size, and object number on detection accuracy. The quality of detection in the YOLO-based network was found to be significantly affected by the initial algorithm hyperparameter combination before the training process. Subsequent training might require different algorithm hyperparameter combinations to improve detection accuracy. To address these issues, a uniform experimental design approach was utilized to identify the optimized algorithm hyperparameter combination (OAHC) for the YOLO-based network. This OAHC was then integrated into the YOLO-based–OAHC model, enhancing the automatic identification and counting of various blood cells. Experimental results demonstrated that the YOLO-based–OAHC model exhibited improved detection accuracy compared with previous models, with superior performance in detecting and counting various types of blood cell.

2. Problem Description

Blood is composed of three primary types of cell: WBCs, RBCs, and platelets. WBCs, or leukocytes, are the largest blood cells, with a diameter of 12–15 μm, and typically range from 4500 to 11000 per microliter of blood. These cells are essential for fighting infections. In contrast, RBCs, or erythrocytes, have a diameter of 6–8 μm and are responsible for transporting oxygen to body tissues. Normal RBC counts range from 4.2 to 5.4 million per microliter for females and 4.7 to 6.1 million per microliter for males. Lastly, platelets, or thrombocytes, which aid in blood clotting, have a diameter of 2–3 μm and normally range from 150000 to 450000 per microliter. Medical professionals often use a complete blood count to assess overall health conditions, as highlighted in studies by Habibzadeh *et al.*[12] and Cruz *et al.*[13] Traditional manual blood cell counting systems that use hemocytometers are time-consuming and prone to high error rates due to the vast number of blood cells. Additionally, the accuracy of these systems heavily depends on the skill level of the clinical laboratory analyst.[14,15] Therefore, an automated process to detect and count different blood cells from smear images can considerably enhance

the efficiency and accuracy of the counting process. Deep-learning-based artificial intelligence models have the potential to be a valuable tool for medical laboratory personnel in identifying and counting various blood cells.

In this study, we utilized the BCCD dataset,[7] a publicly available collection of annotated blood cell images. The BCCD dataset, though small-scale, contains 364 annotated smear images specifically for blood cell detection. It includes three types of blood cell: RBCs, WBCs, and platelets, with each JPEG smear image measuring 640 pixels by 480 pixels. The dataset comprises a total of 4888 labels across the three types: 372 WBCs, 4155 RBCs, and 361 platelets. Figure 1 shows a representative image of blood cell smears, illustrating that platelets are approximately 20% of the diameter of an RBC, while WBCs are about twice the diameter of an RBC. The diameter ratio of the blood cells is 0.2:1:2 for platelets, RBCs, and WBCs, respectively.

3. Methods

The research methodology comprised several key steps. Below are the specific steps involved in the process.

3.1. Collection and processing of microscopic smear images of blood cells

The BCCD dataset provides 364 annotated microscopic smear images, each with dimensions of 640 by 480 pixels in JPEG format. For the purpose of detecting and counting different blood cells, 291 images (80% of the total) were randomly selected as the training set, while the remaining 73 images were designated as the test set. Ground truth labels were generated for both the training set and the test set to evaluate the accuracy of supervised learning techniques. To ensure compatibility with the YOLO-based network and to efficiently detect objects, each image was resized to 320 × 320 × 3, where 3 represents the number of color channels.

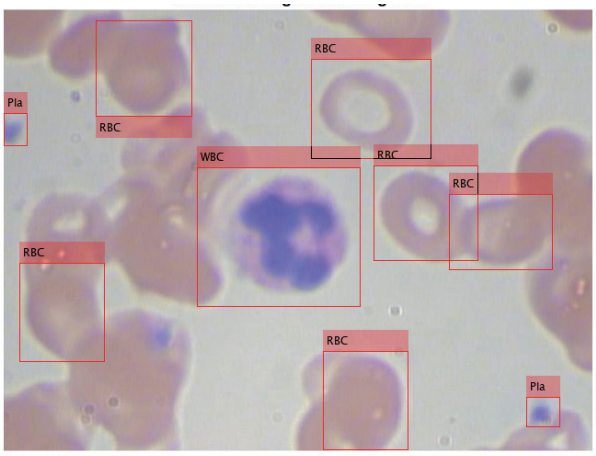

Fig. 1. (Color online) Representative image of blood cell smears.

3.2. Selection of the YOLO-based network and its algorithm hyperparameters

Bochkovskiy *et al.*[16] introduced a YOLO-based algorithm, an advanced object detection model with several key improvements. The YOLO-based architecture combines the CSPDarknet53 backbone, SPP module, PANet path-aggregation neck, and anchor-based head. This enhanced architecture provides improved efficiency and accuracy through advanced training and postprocessing techniques. Consequently, the YOLO-based network was chosen for this study to detect and count blood cells owing to its superior performance.

To achieve high accuracy in detecting images with the YOLO-based network, selecting the appropriate combination of algorithm hyperparameters before the training process is essential. In this study, the following algorithm hyperparameters were selected for the YOLO-based network:

1. InitialLearnRate: initial learning rate during training;
2. LearnRateDropPeriod: number of learning rate drop periods;
3. GradientDecayFactor: decay rate of gradient moving average for Adam solver;
4. SquaredGradientDecayFactor: decay rate of squared gradient moving average for Adam solver;
5. L2Regularization: factor for L2 regularization;
6. MiniBatchSize: size of mini-batch at each iteration.

Additionally, the optimizer was set to 'Adam', with the following training options:

1. MaxEpochs: maximum number of training epochs, set to 50;
2. LearnRateDropFactor: factor by which the learning rate drops, set to 0.5;
3. LearnRateSchedule: schedule for dropping the learning rate during training, set to 'piecewise';
4. LearnRate: rate adjusted by multiplying the learning rate from the previous period by LearnRateDropFactor after every LearnRateDropPeriod.

3.3. Design of algorithm hyperparameter combinations using a uniform experimental design method

The uniform experimental design (UED) method, introduced by Fang,[17] uses space-filling designs to create experimental points that are uniformly distributed across a continuous design parameter space. Unlike methods that focus on comparable orderliness, UED prioritizes uniform dispersion, thereby minimizing the number of experiments needed to gather all necessary information.

In this study, the YOLO-based network is configured with six algorithm hyperparameters: InitialLearnRate, LearnRateDropPeriod, GradientDecayFactor, SquaredGradientDecayFactor, L2Regularization, and MiniBatchSize. To achieve a uniform layout and reduce the number of required experiments, the the $U_{11}(11^6)$ of an uniform experimental design was employed. Consequently, the eleven algorithm hyperparameter combinations derived from the $U_{11}(11^6)$ uniform experimental design were used in the YOLO-based network to detect and quantify various blood cells in microscopic smear images.

3.4. Conduct of uniform layout detection experiments using the YOLO-based network to record detection performances

The recorded results for blood cell detection in the training and test sets included the following:

1. Mean average precision (*mAP*): recorded for each experimental run;
2. Average *mAP*: calculated across three independent runs;
3. *mAP* standard deviation: determined from the three independent runs.

Average precision (*AP*) is the area under the precision–recall curve for a given class. In information retrieval tasks, precision measures the relevance of the results, calculated as the positive predictive value (true positives divided by the sum of true positives and false positives). Recall (sensitivity) measures the true positive rate, calculated as true positives divided by the sum of true positives and false negatives. *mAP* is derived by calculating *AP* for each class and then averaging the *AP* values across all classes.

3.5. Use of the YOLO-based–OAHC model to explore detection accuracy and count various blood cells

The OAHC obtained from the $U_{11}(11^6)$ uniform experimental design achieved the highest average *mAP* across three independent runs on the test set. This OAHC was integrated into the YOLO-based network, forming the YOLO-based–OAHC model. The YOLO-based–OAHC model was then employed to detect and count different blood cells.

3.6. Analysis of the importance of algorithm hyperparameters in the YOLO-based–OAHC model using multiple regression analysis

Multiple regression analysis is a statistical method for investigating the relationship between a dependent variable and multiple independent variables. The aim is to determine the extent to which the variation in dependent variable can be explained by the independent variables. In this study, multiple regression analysis was utilized to identify the algorithm hyperparameters that significantly impact the most crucial feature of the YOLO-based–OAHC model: its ability to accurately detect various types of blood cell in microscopic smear images.

4. Results

The YOLO-based–OAHC model was developed by integrating the YOLO-based network with a refined algorithm hyperparameter configuration to improve feature extraction for detecting and quantifying various blood cells in smear images. To train the YOLO-based–OAHC model, a training dataset consisting of smear images depicting various blood cells from the BCCD dataset was used. The model's performance was evaluated on a test datas*et, al*so containing smear images of various blood cells from the same BCCD dataset. Experiments were performed on a computer with an Intel i7 CPU and a TUF-RTX3090-24G-GAMING GPU. The system utilized Matlab R2025, developed by MathWorks, along with its corresponding toolboxes.

4.1. Preparation of image data

The experimental evaluation of the YOLO-based network's ability to detect and count various blood cells utilized both the training and test sets of microscopic smear images. A total of 364 labeled microscopic smear images from the BCCD dataset were used for object detection. For each experiment, 291 images (80% of the total) were randomly selected as the training dataset, while the remaining 73 images (20% of the total) were reserved for testing the model's ability to identify and count different blood cells. To assess detection accuracy, ground truth labels were established for both the training and test datasets. To conform to the YOLO-based network and efficiently detect objects, each image was resized to 320 × 320 × 3 dimensions, where 3 represents the number of color channels.

The data augmentation techniques implemented in this study included the random scaling of both the image and its associated box labels, the horizontal flipping of the image and its corresponding box labels, and color modifications. These augmentation strategies were applied exclusively to the training dataset to enhance the diversity of the training data without increasing the number of labeled samples. The test dataset was left unmodified to ensure it represented the original data, providing an unbiased evaluation of the model's performance. Figure 2 illustrates an example of a smear image of various blood cells after data augmentation.

4.2. Design of algorithm hyperparameter combinations using a uniform experimental design method for the YOLO-based network

This study's algorithm hyperparameters were classified into two groups: fixed values and optimized values. The fixed values comprised an optimizer of 'Adam', MaxEpochs set to 50, LearnRateDropFactor set to 0.5, and a LearnRateSchedule of 'piecewise'. The YOLO-based network had six algorithm hyperparameters that were optimized in this study, namely, InitialLearnRate, LearnRateDropPeriod, GradientDecayFactor, SquaredGradientDecayFactor, L2Regularization, and MiniBatchSize.

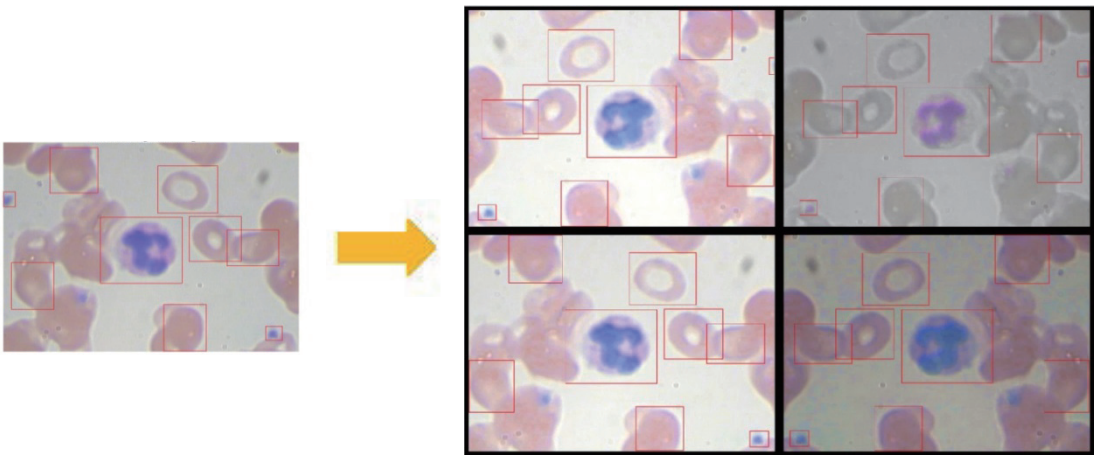

Fig. 2. (Color online) Sample smear image depicting various blood cells after data augmentation.

To maintain a uniform layout and minimize the number of experiments required for the six algorithm hyperparameters, the $U_{11}(11^6)$ of a uniform experimental design was implemented. Consequently, the YOLO-based network was subjected to eleven algorithm hyperparameter combinations, designed through the $U_{11}(11^6)$ uniform layout, to detect and count various blood cells in microscopic smear images. Table 1 shows the uniform experimental design of $U_{11}(11^6)$.

We tested several levels of hyperparameters in our experiment. For the hyperparameter 'InitialLearnRate' (Factor A), we tested two levels, 10^{-4} and 10^{-3}. For 'LearnRateDropPeriod' (Factor B), we tested three levels, 10, 15, and 20. 'GradientDecayFactor' (Factor C) was tested at five levels, 0.9, 0.8, 0.7, 0.6, and 0.5. Similarly, for 'SquaredGradientDecayFactor' (Factor D), we tested three levels, 0.999, 0.99, and 0.9. For 'L2Regularization' (Factor E), we tested five levels, 0.0005, 0.0004, 0.0003, 0.0002, and 0.0001. Owing to GPU memory limitations, 'MiniBatchSize' (Factor F) was tested at five levels, 4, 6, 8, 10, and 12. To adapt to the 11 levels of $U_{11}(11^6)$, we used cyclic level processing. Table 2 shows the factors and levels for the YOLO-based network.

Table 1
$U_{11}(11^6)$ of the uniform experimental design.

Experiment	Factors					
no.	A	B	C	D	E	F
1	1	2	3	5	7	10
2	2	4	6	10	3	9
3	3	6	9	4	10	8
4	4	8	1	9	6	7
5	5	10	4	3	2	6
6	6	1	7	8	9	5
7	7	3	10	2	5	4
8	8	5	2	7	1	3
9	9	7	5	1	8	2
10	10	9	8	6	4	1
11	11	11	11	11	11	11

Table 2
Factors and levels for the YOLO-based network.

Level	Factors					
	A	B	C	D	E	F
1	10^{-4}	10	0.9	0.999	0.0005	4
2	10^{-3}	15	0.8	0.99	0.0004	6
3	10^{-4}	20	0.7	0.9	0.0003	8
4	10^{-3}	10	0.6	0.999	0.0002	10
5	10^{-4}	15	0.5	0.99	0.0001	12
6	10^{-3}	20	0.9	0.9	0.0005	4
7	10^{-4}	10	0.8	0.999	0.0004	6
8	10^{-3}	15	0.7	0.99	0.0003	8
9	10^{-4}	20	0.6	0.9	0.0002	10
10	10^{-3}	10	0.5	0.999	0.0001	12
11	10^{-4}	15	0.9	0.99	0.0005	4

PS, A: InitialLearnRate, B: LearnRateDropPeriod, C: GradientDecayFactor, D: SquaredGradientDecayFactor, E: L2Regularization, F: MiniBatchSize.

Table 3 shows the eleven algorithm hyperparameter combinations derived by merging the values from Tables 1 and 2. These combinations were employed in the YOLO-based network to detect and count various blood cells in smear images.

4.3. Conduct of uniform layout detection experiments using the YOLO-based network to record detection performances

We utilized the eleven algorithm hyperparameter combinations presented in Table 3 for experimental runs in the training and test sets of the YOLO-based network. To evaluate the network's performance in detecting various blood cells in smear images, Table 4 shows the *mAP* achieved in a single run, as well as the average *mAP* and standard deviation (*SD*) from three independent experimental runs. As shown in Table 4, experiment 4 attained significantly high average *mAP* values of 0.9893 in the training set and 0.8588 in the test set, accompanied by low standard deviations of 0.00243 and 0.01091, respectively. This experiment utilized a hyperparameter combination for the YOLO-based network that exhibited excellent performance in detecting various types of blood cell in smear images. The hyperparameter configuration for Experiment 4 consisted of an InitialLearnRate of 10^{-3}, a LearnRateDropPeriod of 15, a GradientDecayFactor of 0.9, a SquaredGradientDecayFactor of 0.9, an L2Regularization of 0.0005, and a MiniBatchSize of 6. Additionally, it was accompanied by a fixed optimizer of 'Adam', MaxEpochs set to 50, LearnRateDropFactor set to 0.5, and a LearnRateSchedule of 'piecewise'.

Figure 3 shows the *mAP*-3 outcome from experiment 4, as reported in Table 4. The results showcase the ability of the YOLO-based network to detect different types of blood cell in microscopic smear images, both in the training and test sets. Experiment 4 achieved an *mAP*-3 score of 0.9900 on the training set, with individual *AP* scores of 0.9966 for WBCs, 0.9899 for RBCs, and 0.9836 for platelets, as depicted in Table 4 and Fig. 3(a). On the other hand, as shown

Table 3
Eleven algorithm hyperparameter combinations for the YOLO-based network.

Experiment	Factors					
no.	A	B	C	D	E	F
1	10^{-4}	15	0.7	0.99	0.0004	12
2	10^{-3}	10	0.9	0.999	0.0003	10
3	10^{-4}	20	0.6	0.999	0.0001	8
4	10^{-3}	15	0.9	0.9	0.0005	6
5	10^{-4}	10	0.6	0.9	0.0004	4
6	10^{-3}	10	0.8	0.99	0.0002	12
7	10^{-4}	20	0.5	0.99	0.0001	10
8	10^{-3}	15	0.8	0.999	0.0005	8
9	10^{-4}	10	0.5	0.999	0.0003	6
10	10^{-3}	20	0.7	0.9	0.0002	4
11	10^{-4}	15	0.9	0.99	0.0005	4

PS, A: InitialLearnRate, B: LearnRateDropPeriod, C: GradientDecayFactor, D: SquaredGradientDecayFactor, E: L2Regularization, F: MiniBatchSize.

Table 4
mAP, average *mAP,* and *SD* obtained by the YOLO-based network for detecting various blood cells in smear images, using each algorithm hyperparameter combination from Table 3 across three independent experimental runs.

Experiment no.	Dataset	*mAP*-Experiment no.			Average *mAP*	*SD*
		mAP-1	*mA*P-2	*mAP*-3		
1	Training set	0.4902	0.4953	0.4936	0.4930	0.00260
	Test set	0.4898	0.4983	0.4945	0.4942	0.00426
2	Training set	0.8685	0.8358	0.8591	0.8545	0.01684
	Test set	0.8473	0.8264	0.8567	0.8435	0.01551
3	Training set	0.4939	0.5008	0.5006	0.4984	0.00393
	Test set	0.4935	0.4977	0.4734	0.4882	0.01299
4	Training set	0.9866	0.9913	0.9900	0.9893	0.00243
	Test set	0.8504	0.8548	0.8711	0.8588	0.01091
5	Training set	0.9125	0.894	0.9106	0.9057	0.01018
	Test set	0.8475	0.8355	0.8245	0.8358	0.01150
6	Training set	0.9357	0.9507	0.9408	0.9424	0.00763
	Test set	0.8143	0.8372	0.839	0.8302	0.01377
7	Training set	0.5288	0.5094	0.5095	0.5159	0.01117
	Test set	0.5053	0.4999	0.4995	0.5016	0.00324
8	Training set	0.9312	0.9462	0.9520	0.9431	0.01073
	Test set	0.8194	0.8248	0.8335	0.8259	0.00711
9	Training set	0.4809	0.4528	0.4820	0.4719	0.01655
	Test set	0.4574	0.4640	0.4801	0.4672	0.01168
10	Training set	0.9939	0.9925	0.9888	0.9917	0.00264
	Test set	0.8570	0.8409	0.8397	0.8459	0.00966
11	Training set	0.9019	0.8881	0.9015	0.8972	0.00785
	Test set	0.8189	0.8035	0.8367	0.8197	0.01661

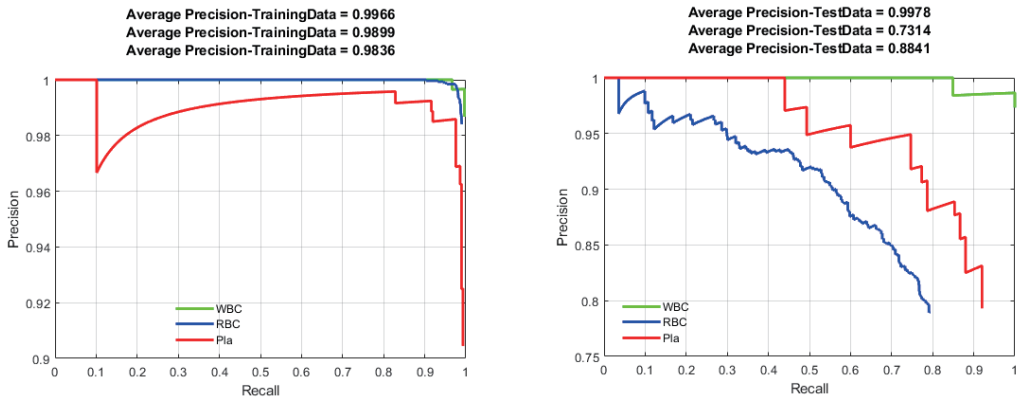

(a) (b)

Fig. 3. (Color online) *mAP*-3 result from experiment 4 as reported in Table 4, showcasing the performance of the YOLO-based network in detecting various blood cells in microscopic smear images, for both the training and test sets. (a) *AP*s computed on the training set. (b) *AP*s computed on the test set.

in Table 4 and Fig. 3(b), experiment 4 achieved an *mAP*-3 score of 0.8711 on the test set, with individual *AP* scores of 0.9978 for WBCs, 0.7314 for RBCs, and 0.8841 for platelets. The WBC class exhibits a higher detection accuracy owing to its clear characteristics and a larger size than other blood cells in the BCCD dataset, with a diameter ratio of 2:1:0.2 for WBCs, RBCs, and platelets, respectively. In contrast, the smaller size of platelets and their tendency to overlap with RBCs without clear boundaries result in a lower detection accuracy for this class. Similarly, the detection accuracy for RBCs is relatively low owing to the abundance of RBCs and their tendency to overlap with other cells.

4.4. Analysis of the importance of algorithm hyperparameters of the YOLO-based–OAHC model using a multiple regression analysis approach for exploring the detection accuracy in microscopic smear images of blood cells

Experiment 4 of the $U_{11}(11^6)$ layout achieved the highest average *mAP* in three independent runs on the test set by utilizing the appropriate algorithm hyperparameter combination. The optimized algorithm hyperparameter combination was then incorporated into the YOLO-based network, resulting in the YOLO-based–OAHC model. This model was subsequently utilized to detect various blood cells. To determine the algorithm hyperparameters that significantly affected the YOLO-based–OAHC model's most critical feature, which is its ability to detect different types of blood cell accurately in microscopic smear images, we employed multiple regression analysis. Table 5 shows the estimated coefficients, *p*-values, and model statistic values for the multiple regression model.

In the multiple regression model, the estimated coefficients are the numerical values that determine the relationship between the dependent variable and the independent variables. *P*-values, on the other hand, indicate the significance of the coefficients and whether they are statistically significant or not. On the basis of the information provided in Table 5, it appears that a study has been conducted to analyze the effects of factors A (InitialLearnRate), C (GradientDecayFactor), and D (SquaredGradientDecayFactor) on some outcome of interest. The *p*-values for these factors have been reported, and it has been noted that any factor with a *p*-value

Table 5
Estimated coefficients, *p*-values, and model statistic values for the multiple regression model.

Factor (algorithm hyperparameter)	Estimated coefficient	*p*-value
(Intercept)	3.215	0.006384
A (InitialLearnRate)	−3201.6	0.014169
C (GradientDecayFactor)	0.53598	0.014405
D (SquaredGradientDecayFactor)	−2.9049	0.011875
F (MiniBatchSize)	−0.017744	0.062851
$A \times D$	3456.1	0.011935
Number of observations: 11, Error degrees of freedom: 5		
Root mean squared error: 0.0535		
R-squared: 0.954, Adjusted R-squared: 0.908		
F-statistic vs constant model: 20.6, *p*-value = 0.00237		

smaller than 0.05 is considered statistically significant. The statistics of a model provide valuable information regarding the model's goodness of fit, including the R-squared value, which quantifies the proportion of variation in dependent variable that can be accounted for by the independent variables. In this study, the R-squared value was 0.954, which suggests an excellent fit of the model. Additionally, the *p*-value of the model was 0.00237, which indicates a significant relationship between the independent and dependent variables in the multiple regression model. Therefore, on the basis of these results, it can be inferred that the model is highly appropriate, as reflected by the high R-squared value, and the relationship between the independent and dependent variables is statistically significant, as supported by the low *p*-value.

The multiple regression analysis conducted on the six selected factors revealed that three factors, namely, A (InitialLearnRate), C (GradientDecayFactor), and D (SquaredGradientDecayFactor), were statistically significant in determining the detection accuracy of the YOLO-based–OAHC model for detecting various blood cells in microscopic smear images.

5. Discussion

Can the accuracy of object detection in identifying various blood cells in microscopic smear images be affected by image size? The platelets, RBCs, and WBCs have a diameter ratio of 0.2:1:2. In Fig. 1, the blood cells are depicted in terms of their quantity and size. RBCs are the most numerous but often overlap, platelets are the smallest and least abundant, and WBCs are the largest but the least numerous. To evaluate the detection accuracy of the YOLO-based–OAHC model, images were processed at sizes of 320 × 320 × 3 and 512 × 512 × 3. Table 6 shows the comparison of results obtained using the YOLO-based–OAHC model for these image sizes. The average *mAP* for the test set using 320 × 320 × 3 images was 0.8588, slightly higher than the 0.8564 obtained with 512 × 512 × 3 images. For 320 × 320 × 3 images, the *mAP*-3 for the test set was 0.8711, with *AP*s for WBCs, RBCs, and platelets at 0.9978, 0.7314, and 0.8841, respectively. In contrast, for 512 × 512 × 3 images, the *mAP*-1 was 0.8639, with *AP*s for WBCs, RBCs, and platelets at 0.9891, 0.7384, and 0.8643, respectively. The results show that detection accuracy for different blood cells using the YOLO-based-OAHC model is not significantly affected by varying the input image size between 320 × 320 × 3 and 512 × 512 × 3. Moreover, using smaller image sizes for training can lead to considerable savings in training time.

Table 6
Comparison of results obtained using the YOLO-based–OAHC model at image sizes of 320 × 320 × 3 and 512 × 512 × 3.

Image size	Dataset	*mAP*-Experiment no.			Average *mAP*	*SD*
		mAP-1	*mAP*-2	*mAP*-3		
320 × 320 × 3	Training set	0.9866	0.9913	0.9900	0.9893	0.00243
	Test set	0.8504	0.8548	0.8711	0.8588	0.01091
512 × 512 × 3	Training set	0.9928	0.9939	0.9911	0.9926	0.00141
	Test set	0.8639	0.8424	0.863	0.8564	0.01216

Is it necessary to select a specific algorithm hyperparameter combination for object detection? In this study, we highlight the importance of selecting the correct combination of algorithm hyperparameters for accurately detecting different types of blood cell in microscopic smear images using the YOLO-based network. As shown in Table 4, the average *mAP*s for experiments 1, 3, 7, and 9 were below 0.5 for the test set, primarily due to suboptimal algorithm hyperparameter selections. These findings indicate that an improper combination of algorithm hyperparameters cannot accurately detect blood cells in microscopic smear images. Consequently, we employed a uniform experimental design methodology to determine the optimal algorithm hyperparameter combination for detecting blood cells using the YOLO-based network.

Below are the performance comparisons of deep learning methods on detection accuracy for various blood cells in microscopic smear images. Alam and Islam[4] found that on the test set, the Tiny YOLO, VGG-16 with YOLO, ResNet50 with YOLO, InceptionV3 with YOLO, and MobileNet with YOLO models achieved *mAP*s of 0.6236, 0.7132, 0.7437, 0.6826, and 0.5207, respectively. Note that although Alam and Islam[4] utilized the BCCD database, they altered the data, used different image sizes, and applied varying numbers of training and the test sets. Therefore, direct comparisons of detection accuracy across different deep learning models are not reasonable. Additionally, researchers frequently use their own datasets for detecting and counting blood cells, which complicates comparisons between studies. Notably, the Resnet50-SSD model using a 512 × 512 × 3 input image size, as obtained by Chen *et al.*[6], achieved an average *mAP* of 0.7747. In contrast, the YOLO-based–OAHC model using a 512 × 512 × 3 input image size achieved an average *mAP* of 0.8564 in this study. These results indicate that the YOLO-based–OAHC model demonstrated a higher detection accuracy than the Resnet50-SSD model reported by Chen *et al.* [6] on the test set of blood cell images. Table 7 presents a comparison between the results obtained using the YOLO-based-OAHC model with an input image size of 512 × 512 × 3 and the Resnet50-SSD model with an input image size of 512 × 512 × 3.

Below is the counting performance of the YOLO-based–OAHC model for various blood cells in microscopic smear images. The model achieved the *mAP*-3 of 0.8711 on the test set with an input image size of 320 × 320 × 3, as shown in Table 6. The test set comprised 73 images and 994 ground truth labels, which included 73 WBCs, 846 RBCs, and 75 platelets. The YOLO-based–OAHC model detected and counted 75 WBCs with an accurrrcy higher than 100%. This high

Table 7
Comparison of results obtained using the YOLO-based–OAHC model with input image size of 512 × 512 × 3 and the Resnet50-SSD model with input image size of 512 × 512 × 3.

Model	Image size	Dataset	*mAP*-Experiment no.			Average *mAP*
			mAP-1	*mAP*-2	*mAP*-3	
YOLO-based-OAHC	512 × 512 × 3	Training set	0.9928	0.9939	0.9911	0.9926
		Test set	0.8639	0.8424	0.863	0.8564
Resnet50-SSD	512 × 512 × 3	Training set	0.7899	0.7866	0.7808	0.7858
		Test set	0.7763	0.7772	0.7707	0.7747

accuracy is due to the larger size and clear characteristics of WBCs, combined with the number of ground truths being lower than the actual count. For RBCs, the model detected 864 RBCs, surpassing the ground truth count of 846 and resulting in an accuracy higher than 100%. The model also accurately detected and counted 88 platelets, again exceeding the ground truth due to the limited number of labeled platelets. Figure 4 illustrates the ground truth labels of blood cells and the detected blood cells labeled by the YOLO-based–OAHC model. Detection and counting accuracy can be further improved by selecting areas with a more even distribution of blood cells in microscopic smear images.

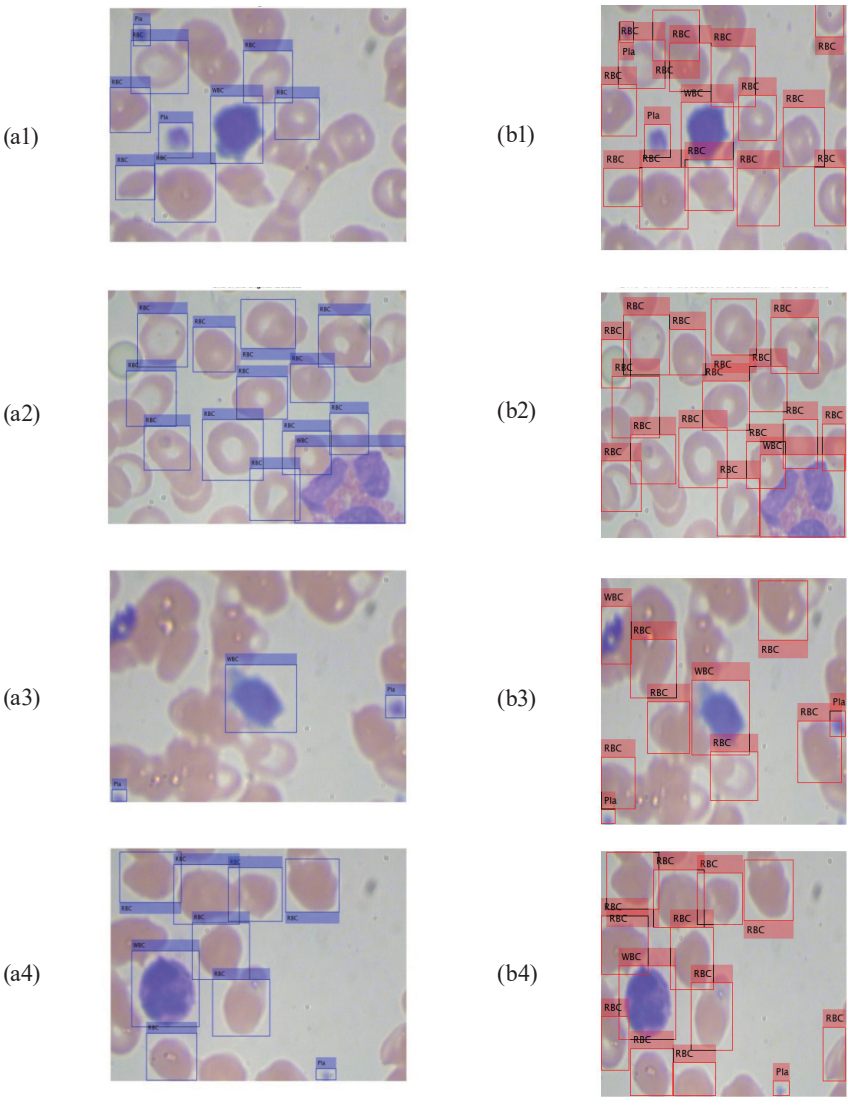

Fig. 4. (Color online) Ground truth labels of blood cells (a1–a4) and the labeled blood cells (b1–b4) detected by the YOLO-based–OAHC model.

6. Conclusions

The proposed YOLO-based–OAHC model in this study demonstrated enhanced accuracy in detecting and counting blood cells, especially WBCs and platelets, in microscopic smear images. The first significant contribution of this study is the finding that using different image sizes (320 × 320 × 3 and 512 × 512 × 3) does not significantly affect object detection accuracy. The model with a 320 × 320 × 3 input image size achieved the average *mAP* of 0.8588 in three independent experiments, slightly outperforming the 512 × 512 × 3 input size, which had the average *mAP* of 0.8564 on the test set. The second contribution is the demonstration that the YOLO-based–OAHC model can achieve high detection accuracy by utilizing an optimal combination of algorithm hyperparameters. The optimal hyperparameter combination obtained through the uniform experimental design method resulted in the average *mAP* of 0.8588 with a 320 × 320 × 3 input image size on the test set. In contrast, suboptimal hyperparameter selections resulted in average *mAP*s of less than 0.5 for experiments 1, 3, 7, and 9, as shown in Table 4. The third contribution is showing that an improved object detection model can identify new objects exceeding the ground truth labels on the test set. The YOLO-based–OAHC model proposed in this research detected and counted WBCs, RBCs, and platelets with an accuracy highr than 100%, as the actual number of these cells on the test set exceeded the number of ground truth labels.

Acknowledgments

This study was funded by the National Science and Technology Council, Taiwan, R.O.C., under Grants NSTC 112-2221-E-037-004-MY3 and NSTC 113-2221-E-153-002-MY2. This work was also supported in part by the NPUST-KMU joint research project (NPUST-KMU-115-P006), Yuan's General Hospital (ST112001), and Precision Sports Medicine and Health Promotion Center, Kaohsiung Medical University (KMU-TC115A06-1), Kaohsiung 807, Taiwan.

References

1. B. George-Gay and K. Parker: J. Perianesth. Nurs. **18** (2003) 96. https://doi.org/10.1053/jpan.2003.50013
2 S. W. Lockley, L. K. Barger, N. T. Ayas, J. M. Rothschild, C. A. Czeisler, and C. P. Landrigan: Jt. Comm. J. Qual. Patient Saf. **33** (2007) 7. https://doi.org/10.1016/S1553-7250(07)33109-7
3 G. Drałus, D. Mazur, and A. Czmil: Entropy **23** (2021) 1522. https://doi.org/10.3390/e23111522
4 M. M. Alam and M. T. Islam: Healthc. Technol. Lett. **6** (2019) 103. https://doi.org/10.1049/htl.2018.5098
5 M. Kim, C. Yan, D. Yang, Q. Wang, J. Ma, and G. Wu: Deep Learning in Biomedical Image Analysis (Academic Press, Cambridge, 2020) Chap. 1.
6 Y. M. Chen, J. T. Tsai, and W. H. Ho: BMC Bioinf. **22** (2022b) 635 https://doi.org/10.1186/s12859-022-05074-2
7 BCCD dataset: https://github.com/Shenggan/BCCD_Dataset (accessed May 2026).
8 Q. Wang, S. Bi, M. Sun, Y. Wang, D. Wang, and S. Yang: PLoS One **14** (2019) e0218808. https://doi.org/10.1371/journal.pone.0218808
9 M. R. Reena and P. M. Ameer: Comput. Biol. Med. **126** (2020) 104034. https://doi.org/10.1016/j.compbiomed.2020.104034
10 Y. M. Chen, F. I. Chou, W. H. Ho, and J. T. Tsai: BMC Bioinformatics **22** (2022) 615. https://doi.org/10.1186/s12859-022-04558-5
11 Y. M. Chen, Y. J. Chen, W. H. Ho, and J. T. Tsai: BMC Bioinformatics **22** (2021) 147. https://doi.org/10.1186/s12859-021-04083-x

12 M. Habibzadeh, A. Krzyżak, and T. Fevens: Proc. Int. Conf. Artificial Intelligence and Soft Computing (Springer, 2013) 263–274.
13 D. Cruz, C. Jennifer, and L. C. Valiente: Proc. 2017 IEEE 9th Int. Conf. Humanoid, Nanotechnology, Information Technology, Communication and Control, Environment and Management (IEEE, 2017) 1–7.
14 S. Acharjee, S. Chakrabartty, M. I. Alam, N. Dey, V. Santhi, and A. S. Ashour: Proc. 2016 Int. Conf. Electrical, Electronics, and Optimization Techniques (IEEE, 2016) 525–529.
15 J. Lou, M. Zhou, Q. Li, C. Yuan, and H. Liu: Proc. 2016 9th Int. Congr. Image and Signal Processing, BioMedical Engineering and Informatics (IEEE, 2016) 1391–1396.
16 A. Bochkovskiy, C. Y. Wang, and H. Y. Liao: https://arxiv.org/abs/2004.10934 (accessed May 2026).
17 K. T. Fang: Uniform Design and Uniform Layout (Science Press, Beijing, 1994).